JOURNAL OF TECHNIQUES

Journal homepage*: http://journal.mtu.edu.iq*

RESEARCH ARTICLE - MATERIAL SCIENCE (MISCELLANEOUS)

Influence of Ag₂O Nanoparticles on the Ammonia Gas Sensing Properties of CNT/P3HT Composite Films

Hayder Abdulmeer Abbas[1], Wissem Cheikhrouhou Koubaa[1*]

[1]Centre de Recherche en Numérique de Sfax (CRNS), Faculty of Science of Sfax, University of Sfax, Technopole of Sfax, Tunisia

[*] Corresponding author E-mail: wissem.cheikhrouhou@crns.tn

Article Info.	Abstract
	In this research, the CNT/P3HT and CNT/P3HT@Ag₂O composite films were prepared to be utilized as the ammonia gas sensor. Moreover, the impact of the synthesized composites on ammonia gas sensing and the effect of Ag₂O nanoparticles on the properties of the composites were examined. The layers were analyzed using XRD, AFM, FTIR, and gas sensing analysis, providing insights into their potential for improving ammonia gas sensing. Despite changes in the P3HT to CNT ratios, the XRD analysis of the CNT/P3HT and CNT/P3HT@Ag₂O composite films revealed the same structural properties for the carbon nanotubes. In accordance with the data obtained from the FTIR test of the composite films, characteristic P₃HT bands and various functional groups were detected. As the gas sensing analysis indicated, the sensitivity increased with the increasing ratio of P₃HT to CNT, and the highest sensitivity was achieved by the CNT/P3HT (0.7) sensor. Moreover, the addition of silver oxide further increased the sensitivity. These results suggest that the CNT/P3HT@Ag₂O film sensor is highly sensitive to ammonia gas and can be a promising sensor for the detection of ammonia gas.

1. Introduction

Ammonia (NH₃) is an important component in food and fertilizers and plays a role in the nutrition of land-based organisms. However, it can be damaging if used in excessive quantities. The growth of chemical industries has resulted in an increase in ammonia emissions, which can negatively impact respiratory health and lead to chronic diseases. As a result, there's a large necessity for dependable ammonia detection devices. In this regard, sensors, which are highly sensitive and selective tools, can be adopted for monitoring and controlling this environmental pollutant [1–3]. Many research teams have focused on the creation and enhancement of these ammonia gas sensors. These sensors are often made from nanostructured inorganic materials, which are known for their quick sensitivity and response times. This has led researchers to develop a highly selective ammonia gas sensor using tin-titanium dioxide/reduced graphene oxide/carbon nanotube (Sn-TiO2@rGO/CNT) nanocomposites. At room temperature, the sensor showed high response and selectivity to ammonia where various substances like toluene, dimethylformamide, acetone, ethanol, and methanol were present. Notably, the sensor with a molar ratio of Sn/Ti = 1:10 exhibited the highest response to ammonia [4]. Su et al. developed a new room-temperature NH₃ gas sensor using a ternary nanocomposite film of Pd, tin oxide (SnO₂), and reduced graphene oxide (RGO). Due to the low concentrations of NH₃ gas at room temperature, the sensor demonstrated a strong response. Consequently, it showed better sensitivity than the pristine SnO₂ and SnO₂/RGO nanocomposite films. That is because of its higher conductivity and catalytic activity [5]. Several research teams have focused on the creation of gas sensors using conductive polymers to cut down expenses and streamline the synthesis procedure. Furthermore, polymer–based sensors have several advantages, such as a quick manufacturing process, less energy consumption, and the ability to work with room temperatures [6–9]. Poly (3-hexylthiophene-2, 5-diyl) (P3HT) among the conducting polymers, has been widely analyzed for its usage in gas sensing applications. This is especially evident in detecting ammonia gas [1, 3]. P3HT, being an organic semiconductor, has gained attention due to its notable sensing characteristics and widespread availability [2, 10]. Hence, the application and progress of P3HT in gas sensors have marked a new step in the development of the field. The usage of P3HT clearly developed the performance of the sensors. This makes it a promising material for future gas sensing technologies [10]. Thus, it decreases production costs and improves the performance of the sensors. Khanh et al. successfully fabricated a nanocomposite film for an ammonia gas sensor. This was achieved by using a drop-casting technique. The film was made of P3HT, decreased graphene oxide, and multi-walled carbon nanotubes. It indicated an efficient ammonia detection with a quick response time and high sensitivity [1]. Thereafter, Cheng et al. provided a detailed study on the usage of P3HT in gas sensors. P3HT was indicated for its remarkable sensing characteristics and wide availability. That is why the study proposed that P3HT could improve significantly the performance of polymer field-effect transistor-based gas sensors [10]. Kuo et al. reported the fabrication of an organic-inorganic semiconductor gas sensor for detecting ammonia gas.

Nomenclature & Symbols			
CNT	Carbon Nanotube	ALD	Atomic Layer Deposition
P$_3$HT	Poly(3-Hexylthiophene-2,5-diyl)	ZnO	Zinc Oxide
FTIR	Fourier Transform Infrared Spectroscopy	MWNT	Multi-Walled Nanotubes
XRD	X-Ray Diffraction Analysis	SEM	Scanning Electron Microscope
AFM	Atomic Force Microscopy	η	Sensitivity
rGO	Reduced Graphene Oxide		

That is because the sensor was made from a p-type semiconductor, P$_3$HT, and zinc oxide (ZnO) nanowire array produced by atomic layer deposition (ALD). The P3HT-ZnO nanowires semiconductor illustrated a better sensitivity in comparison with the device composed of the ZnO film and P3HT film. Therefore, the gas sensing device could reach a maximum sensitivity of around 11.58 per ppm [11]. First, we prepared CNT/P3HT composites and examined their influence on the sensing characteristics of ammonia gas. Consequently, the researchers investigated the influence of Ag2O nanoparticles on these sensing properties by preparing CNT/P3HT@Ag2O nanocomposite films. In addition to the preparation and examination of CNT/P3HT composites and CNT/P3HT@Ag2O nanocomposite films, an inclusive analysis of the prepared layers was conducted. This means that the evaluation consisted of the use of X-ray diffraction (XRD), Atomic Force Microscopy (AFM), and Fourier Transform Infrared Spectroscopy (FTIR). By making use of such tools and strategies, we gained a better understanding of the compositional and structural features of the layers, enriching this study on ammonia gas sensing.

2. Experimental Procedure

2.1. Synthesis of P3HT@CNT

First, CNT is soaked in ODCB (dichlorobenzene) of a concentration of 1g/liter, equating to 0.005 grams for 5 ml of dichlorobenzene. This resulted in a dark-colored solution. Alongside, 5 grams per liter of P3HT is mixed in 5 milliliters of chloroform which is equal to P3HT of 0.025 grams, which resulted in a solution that is orange colored. The P3HT solution is then gradually added to the CNT solution in five stages. After each addition, the mixture is dispersed for several minutes to ensure optimal results, culminating in a dark red solution. PET foils are prepared and placed on a mild heater. Given the high coloring power, stickiness, slight toxicity, and volatility of the solution, the foils are covered with a napkin to protect the hands and surrounding environment. The solution is evenly spread on the foil using a spray to achieve a uniform surface. Four samples were synthesized with P3HT:CNT ratios of 0.1, 0.3, 0.5, and 0.7.

2.2. Synthesis of silver oxide

To synthesize silver oxide, 2 grams of silver nitrate are dissolved in 25 milliliters of deionized water. Simultaneously, 0.35 grams of PVP is dissolved as a polymerizing agent in 75 milliliters of deionized water. Once fully dissolved, the silver nitrate solution is added to the PVP solution and left to sit for 10 minutes. Sodium hydroxide is then gradually added until the pH reaches 10. The solution is heated in a bath at 70-80 degrees Celsius for one hour until sediment forms. The solution is then left for 24 hours to cool and allow sedimentation before filtering, washing, and drying the precipitate.

2.3. Preparation of P3HT@CNT@Ag$_2$O

The P3HT to CNT ratio varies and was prepared with ratios of 0.1, 0.3, 0.5, and 0.7. For the preparation of silver oxide layers, a fixed amount of 0.8 mg was added to these ratios in the final solution before being manually sprayed and dried on the PET substrate.

3. Results and Discussion

3.1. XRD analysis

Fig. 1 shows the XRD patterns of pristine P3HT. The P3HT shows a (100) reflection peak around 5.2o, which is known to correspond to a well-organized lamellar structure for this material [12,13]. The further (100) and (200) diffraction peaks indicate crystallinity with edge-on chain orientation [14]. The out-of-plane reflection peak (010) results from π-π interchain stacking [15].

The X-ray diffraction pattern of Ag2O nanoparticles is shown in Fig. 2. This XRD pattern shows several peaks, indicating the presence of a crystalline phase. The most intense peak is located at a 2θ angle of 32.83°, corresponding to the (111) plane of the Ag2O cubic crystal structure. Other peaks are present at 2θ angles of 26.65°, 38.06°, 55.08°, 65.52°, and 68.73°, corresponding to the (110), (200), (220), (311), and (222) planes of the silver oxide crystal structure, respectively. The results of our research are in harmony with the findings presented in earlier scholarly reports [16–18]. Fig. 3 shows the XRD patterns of CNT/P3HT composite films with different P$_3$HT to CNT ratios of 0.1, 0.3, 0.5 and 0.7. A distinct peak, associated with the carbon nanotubes, is noticeable at an approximate angle of 26 degrees. Interestingly, despite the increase in the ratio of P$_3$HT to CNT, there is no significant alteration in the shape, position, or intensity of this observed peak. This observation suggests that the structural properties of the carbon nanotubes remain almost consistent even as the proportion of P$_3$HT increases. The XRD patterns of CNT/P3HT@Ag2O nanocomposite films with different ratios of P$_3$HT to CNT (0.1, 0.3, 0.5, and 0.7) are shown in Fig. 4. The carbon nanotubes have a characteristic peak at around 26 degrees, which is clearly visible in the CNT/P3HT@Ag2O nanocomposites as well as the CNT/P3HT films. The peak does not shift much in either shape, position, or intensity as the amount of P3HT increases. Showing that the carbon nanotubes maintain their structural properties regardless of the P$_3$HT proportion [19].

3.2. Fourier-transform infrared spectroscopy (FTIR)

The FT-IR spectrum of the synthesized CNT/P3HT composite samples, as well as those reinforced with silver oxide nanoparticles (CNT/P3HT@Ag2O), are shown in Fig. 5. Also, Table 1 presents the characteristics of the peaks associated with each sample.
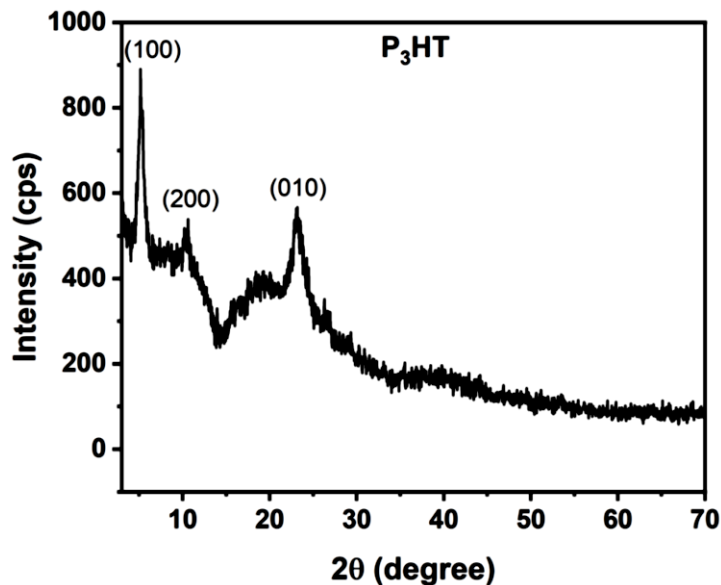
Fig. 1. The XRD pattern of P3HT
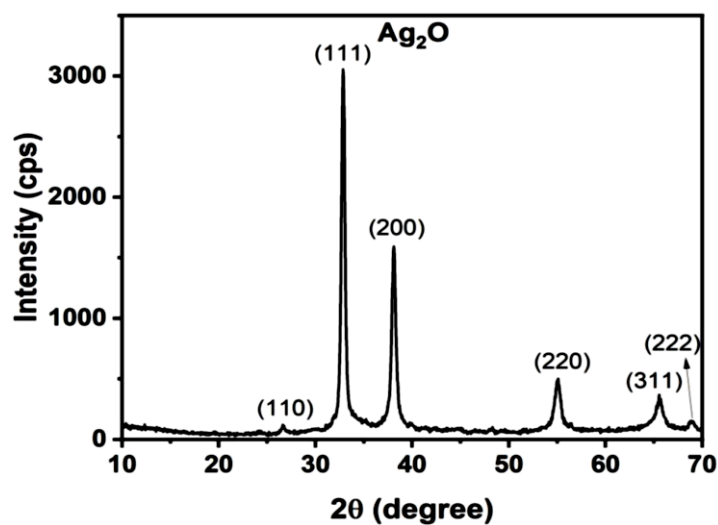
Fig. 2. The XRD pattern of Ag2O nanoparticles
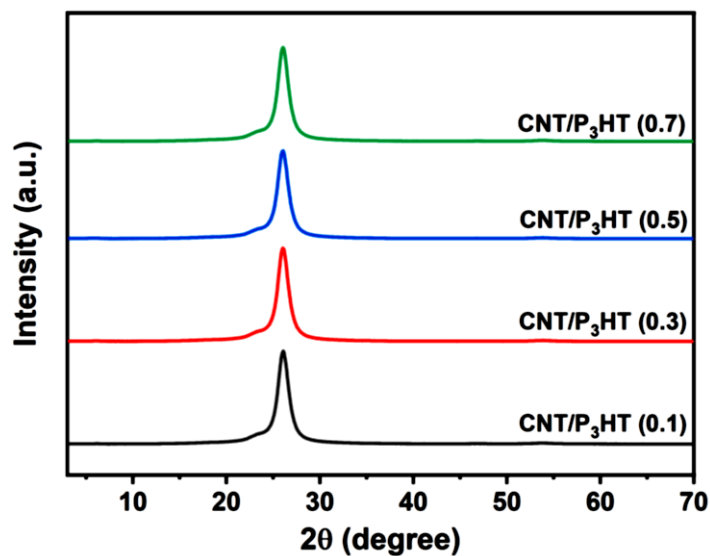
Fig. 3. The XRD pattern of CNT/P3HT films
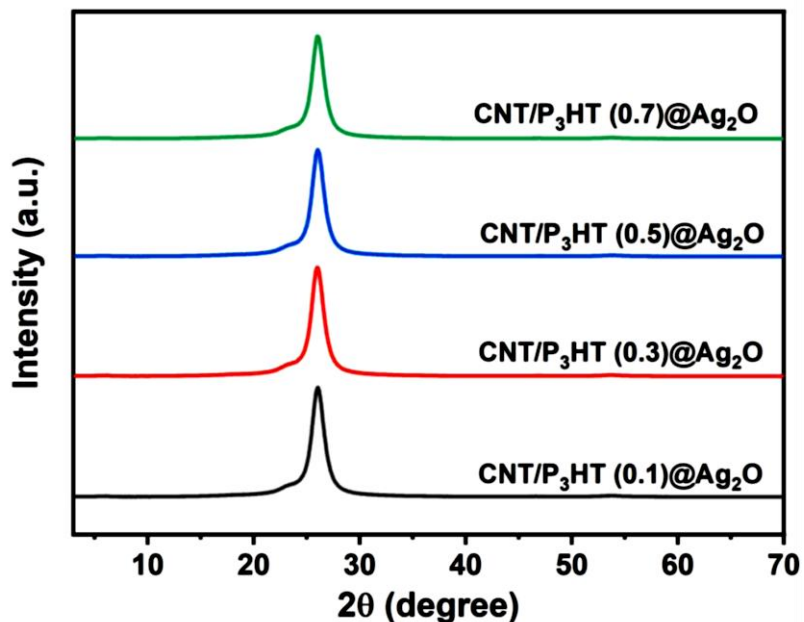
Fig. 4. The XRD pattern of CNT/P3HT@Ag2O nanocomposites
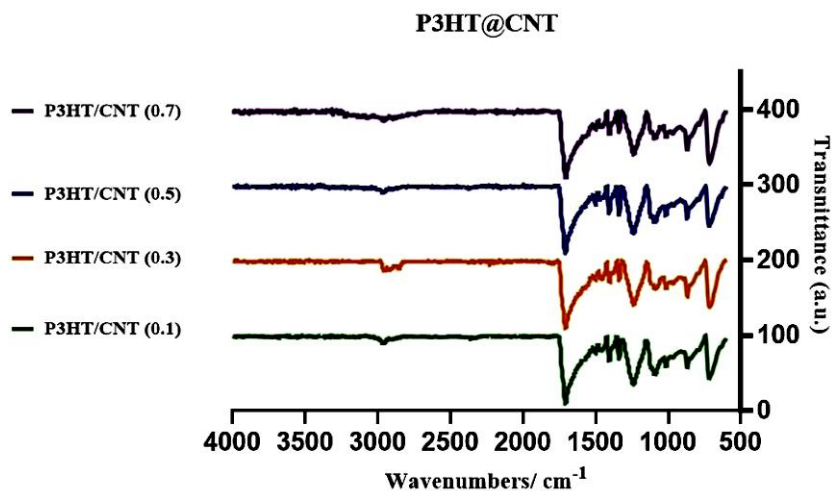
(a)
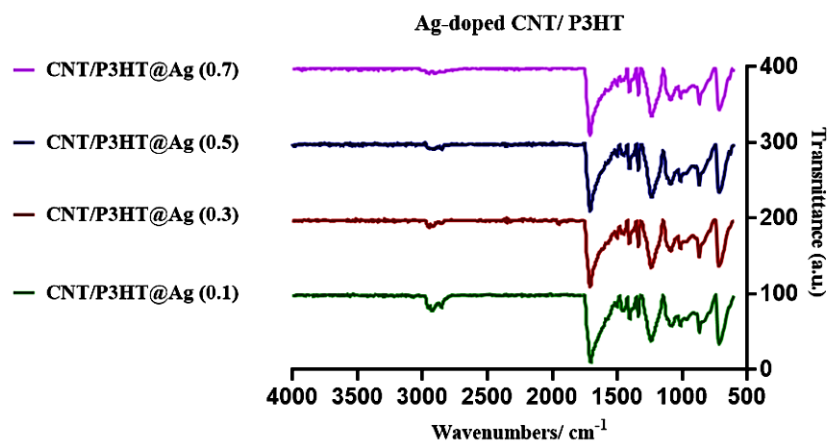
(b)

Fig. 5. FT-IR patterns of (a) CNT/P3HT and (b) CNT/P3HT@ Ag2O thin films at different ratios (0.1, 0.3, 0.5, and 0.7 of P3HT and 0.08 mg/L)

Table 1. Characteristics of peaks of as-prepared CNT/P3HT and CNT/P3HT@Ag2O nanocomposite in FT-IR analysis

Samples	Characteristics of peaks			
	P$_3$HT (0.1)	P$_3$HT (0.3)	P$_3$HT (0.5)	P$_3$HT (0.7)
CNT/P$_3$HT	719.22	716.75	719.90	716.40
	869.48	869.26	870.33	869.94
	1016.46	1015.53	1017.21	1015.27
	1091.93	1089.64	1092.52	1090.87
	1240.14	1238.20	1240.49	1238.28
	1338.99	1338.23	1339.02	1338.78
	1406.33	1405.41	1407.57	1405.73
	1467.98	1461.95	1496.66	1465.48
	1503.74	1503.82	1504.05	1504.18
	1708.18	1707.81	1709.51	1706.65
	2961.85	2956.22	2964.58	2961.13
CNT/P$_3$HT@Ag$_2$O	716.57	717.87	716.90	716.59
	868.89	869.76	869.54	869.41
	1015.14	1015.12	1014.99	1014.45
	1084.55	1091.82	1090.60	1090.44
	1238.84	1237.43	1236.86	1236.60
	1338.60	1337.71	1337.98	1337.57
	1405.24	1406.23	1406.12	1406.12
	1454.78	1455.04	1453.09	1465.68
	1504.76	1504.61	1504.25	1503.68
	1706.17	1709.49	1708.42	1710.50
	2854.67	2923.20	2852.49	
	2924.43	2954.34	2919.66	

As observed in Fig. 5, the CNT/P3HT and CNT/P3HT@Ag2O nanocomposites at varying P3HT concentrations (0.1, 0.3, 0.5, and 0.7) exhibit characteristic P$_3$HT bands [20-22]:

- 716-720 cm^{-1}: due to methylene groups rock,
- 868-870 cm^{-1}: corresponds to the aromatic C-H out-of-plane vibration.
- 1014-1017 cm^{-1}: is related to C–S stretching.
- the peaks at 1503-1505 cm^{-1} and 1338-1466 cm^{-1} are assigned to asymmetric and symmetric thiophene ring C=C stretching vibration (the aryl substituted C=C of the thiophene ring).
- 1337-1339 cm^{-1} is related to methyl bending.
- The bands at 2919-2965 cm^{-1}, and 2852-2955 cm^{-1}: are attributed to the asymmetric C–H stretching vibrations of CH3–/ –CH2- moieties (-CH2 in-plane mode, and -CH3 asymmetry mode), and symmetric C–H stretching vibrations in –CH2– moieties (the -CH2 out-of-plane mode).
- The band at 1014-1017 cm^{-1} is due to the adding of P3HT into the carbon nanotubes (CNT) matrix.

The addition of P3HT into carbon nanotubes increases the intensity of the bands at approximately 1460 cm-1 and 1504 cm-1. This indicates a strong relation between the thiophene ring of the P3HT and the CNT, likely because of van der Waals forces. The bands that are at 1460 cm-1 and 1504 cm-1 are in control of the high intensity. Illustrating a strong inter-molecular interaction between the P3HT and carbon nanotubes as the conjugation is increased in length of the P3HT chain [23]. A report of an increase has been seen through Musumeci et al. [24] in the concentration band at 1460 cm^{-1} and 1504 cm^{-1} for a concentration of 0.1% MWNT in P3HT/MWNT composites. Therefore, the incorporation of MWNTs into the P3HT matrix clearly can improve the electrical features of the composites. As a result, an increased level in the concentration of the bands entitles that the MWNTs are making a strong link with the P3HT matrix. This is due to an increase in the electrical conductivity of the composites [23].

The CNT/P3HT nanocomposites synthesized by this method have peaks related to the P3HT structure, and the C-H stretching vibration peak was slightly changed to higher wavenumbers. The prepared CNT/P3HT thin films with values of P3HT (0.3 and 0.5), reached about 2956.22 cm-1 and 2964.58 cm-1. On the other hand, after adding silver nanoparticles, this wavelength shift value was observed at 0.3 P3HT, which was reported as 2954.34 cm-1 according to Table 1. This slight shift to higher wave numbers can be related to the CH-π interaction between the CNT structure and the P3HT polymer [20].

3.3. Atomic Force Microscopy (AFM)

AFM images of the CNT/P3HT and CNT/P3HT@Ag2O nanocomposites with different concentrations of P3HT, including 0.1, 0.3, 0.5, and 0.7, are presented in Fig. 6. As evidenced by Fig. 6, bright spots are observed, which can be related to the nanotubes protruding from the film sheet [25]. The exposure of tubular structures to the light can result in a higher refractive index, which makes them brighter than the rest of the film sheet. On the other hand, the pristine P3HT films have a low refractive index, and no bright spots are detected for them. The convolution effect of the AFM tip caused the nanotubes to be more curved and compared to the pristine P3HT films which are more uniform in shape, they have more of a jagged shape. As a result, the shape of the protruding nanotubes is affected by the convolution effect of the AFM tip. As Fig. 6-A demonstrates, increasing the amount of P3HT led to better dispersion of carbon nanotubes in the composites. However, in the composite with 0.3 P3HT, agglomeration of carbon nanotubes is still observed in some areas. But a structure with uniform distribution is found for the 0.5 P3HT, implying that the P3HT polymer acts as a binder within the carbon nanotubes, which helps them keep in place and prevents them from clumping together. At higher concentrations of P3HT, the binding effect is stronger, resulting in a more uniform distribution of the carbon nanotubes. The data obtained from this analysis are in good agreement with the data obtained from the scanning electron microscope (SEM) test results. Also, this phenomenon was previously reported by other research groups such as O'Connell et al. used other types of polymers [26] and Giulianini et al. employed scanning probe techniques [27], which confirm the tendency of P3HT to adhere to the surface of carbon nanotube [25]. Incorporation of Ag2O nanoparticles at lower concentrations into the CNT/P3HT nanocomposites gave rise to an enhancement in the distribution of carbon nanotubes. In fact, the presence of the silver nanoparticles improved the interactions between the P3HT molecules and the carbon nanotubes. The silver nanoparticles act as a bridge between the P3HT molecules and the carbon nanotubes, which enhance the binding forces between them. This allows to more uniform distribution or better dispersion of the CNTs at lower concentrations of P3HT; thus, results in the desirable dispersion seen in Fig. 6-B.

3.4. Gas sensing properties

The gas sensing properties of CNT/P3HT@Ag2O films toward the ammonia gas were investigated in a lab-made closed steel chamber, with a LCR meter (Pintek-LCR900, Taiwan), and at a constant voltage of 10 V. Moreover, the HIH4000 and PT100 sensors were respectively employed to record the humidity and the temperature. The resistance of the films was measured over time to monitor the reaction of the sensor with the presence of the gas. The performance parameter which is sometimes referred to as sensitivity (η), is calculated by comparing the resistance of the sensor in the presence of the target gas to its resistance in a gas-free environment. This gives a measure of how much the sensor's resistance shifts in response to the target gas. η is expressed by the following equation [28, 29]

$$\eta \ (\%) = \frac{R - R_0}{R_0} \times 100 \tag{1}$$

Where R_0 is the resistance of the sensor in the presence of the target gas and R is initial resistance in a gas-free environment.

The time dependence of the sensitivities of the CNT/P3HT and CNT/P3HT@Ag2O sensors with different ratios of P3HT to CNT for ammonia gas is shown in Fig. 7. Fig. 7 illustrates a visual representation of how significantly and quickly the sensor responds to ammonia gas as time passes. After the gas is introduced, according to Fig. 7, the sensitivity starts to increase gradually, which indicates that the sensor is responding to the presence of ammonia gas. However, the sensitivity starts to decrease gradually, which indicates that the sensor is recovering in the absence of ammonia gas after the gas is turned off. This clearly demonstrates that these sensors have good sensitivity and good recovery characteristics, making them suitable for use in practical applications where ammonia detection is required. By increasing the ratio of P3HT to CNT from 0.1 to 0.7, it was detected that the sensitivity of sensor CNT/P3HT increases, so sensor CNT/P3HT (0.7) has the highest sensitivity amid these series of samples. Also, by adding silver oxide to the sensor, the sensitivity should be increased, and the CNT/P3HT@Ag2O sensor samples indicated a higher sensitivity compared to the CNT/P3HT sensors. In this series of samples, increasing the ratio of P3HT to CNT increases the sensitivity of the sensor to gas. Among all the sensors, the CNT/P3HT@Ag2O (0.7) sensor has the highest sensitivity. These results suggest that the CNT/P3HT@Ag2O film sensor is sensitive to ammonia gas, as evidenced by the change in sensitivity in response to the presence and absence of the gas.
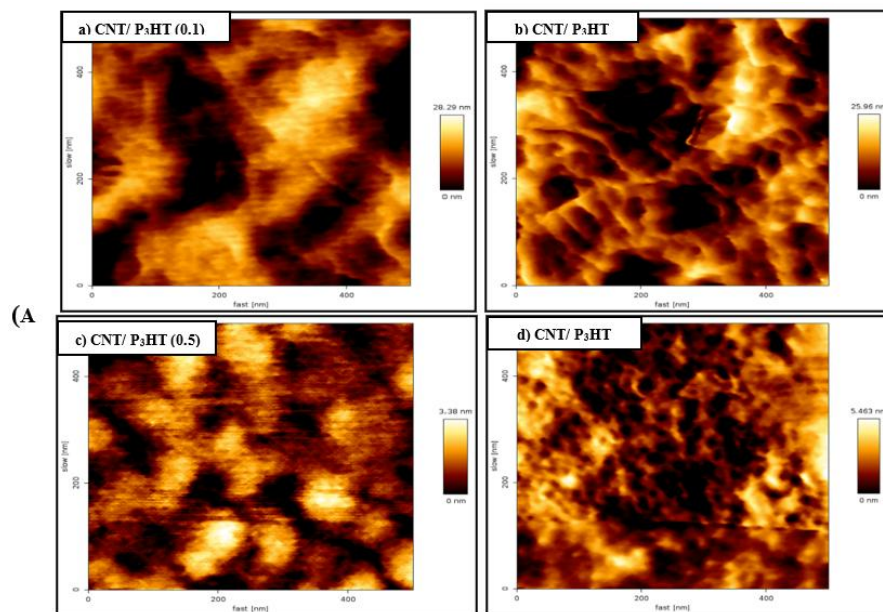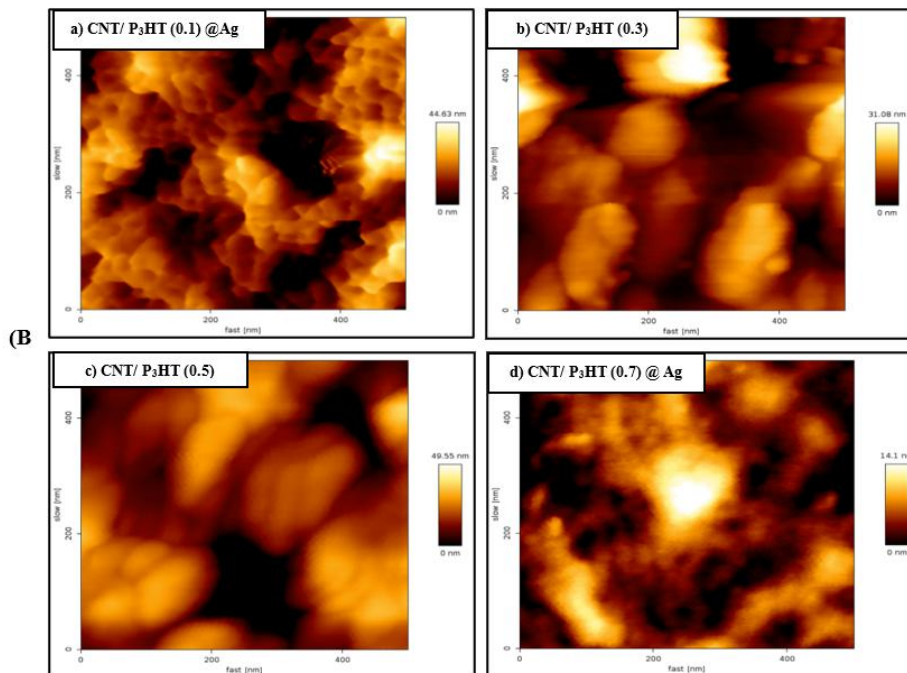
Fig. 6. AFM pictures of (A) prepared thin films with dissimilar P3HT concentrations: (a) CNT/P3HT (0.1), (b) CNT/P3HT (0.3), (c) CNT/P3HT (0.5), and (d) CNT/P3HT (0.7); and (B) CNT/P3HT thin films after doping with silver oxide nanoparticles: (a) CNT/P3HT (0.1) @Ag2O, (b) CNT/P3HT (0.3) @Ag2O, (c) CNT/P3HT (0.5) @Ag2O, and (d) CNT/P3HT (0.7) @Ag2O [dopant amount: 0.08 mg/l].
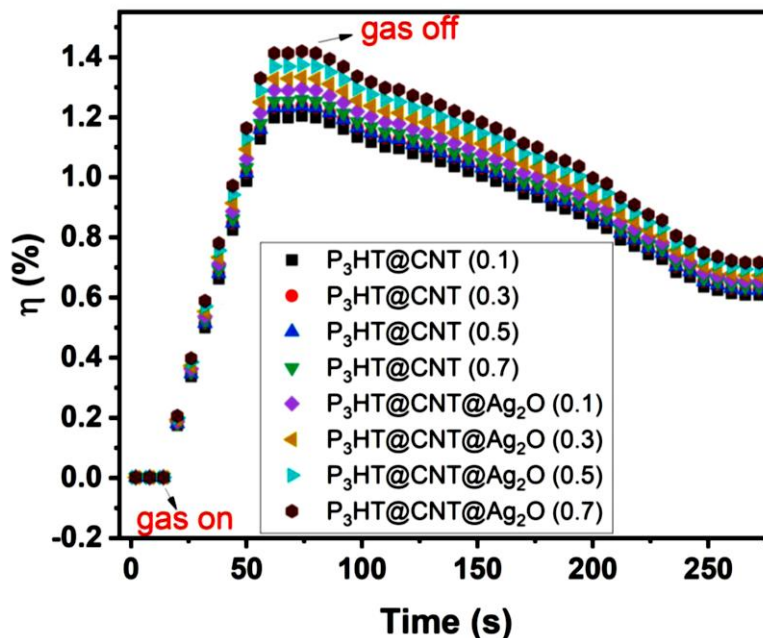
Fig. 7. Gas sensitivity of CNT/P3HT and CNT/P3HT@Ag2O sensors

4. Conclusion

This paper focused on the effectiveness of CNT/P3HT and CNT/P3HT@Ag2O composite films in ammonia gas sensing. It was noticed that the sensitivity of these sensors increased proportionally with the ratio of P$_3$HT to CNT. This sensitivity was later enhanced through the addition of silver oxide, which indicated a positive correlation between the presence of silver oxide and sensor sensitivity. Our study established that these sensors possess commendable sensitivity and recovery features. The recovery features refer to the ability of the sensor to return to its original state after the detection event, which is a significant factor for reusable sensors. These attributes make them suitable for practical applications where consistent and reliable ammonia detection is needed. Among all the sensors tested, the CNT/P3HT@Ag2O (0.7) sensor was distinguished by exhibiting the highest sensitivity. This illustrates that an optimal balance between P3HT and CNT can result in an enhanced sensor performance. These outcomes open new possibilities for the use of such composite films in enhancing ammonia gas sensing capabilities. It paves the way for upcoming research in this field, focusing on how these composite films can be further optimized and potentially integrated into larger systems for environmental monitoring and control.

Acknowledgment

References

[1] Khanh, T. S. T., Trung, T. Q., Giang, L. T. T., Nguyen, T. Q., Lam, N. D., & Dinh, N. N. Ammonia gas sensing characteristic of P3HT-rGO-MWCNT composite films. Applied Sciences, 11(15), 6675, 2021. https://doi.org/10.3390/app11156675.

[2] Han, S., Zhuang, X., Shi, W., Yang, X., Li, L., & Yu, J. Poly (3-hexylthiophene)/polystyrene (P3HT/PS) blends based organic field-effect transistor ammonia gas sensor. Sensors and Actuators B: Chemical, 225, 10-15, 2016. https://doi.org/10.1016/j.snb.2015.11.005.

[3] Lam, M. L., Nguyen, N. D., & Tran, Q. T. Characterization of NH3 sensing properties of P3HT+ rGO+ CNT composite films made by spin-coating. Communications in Physics, 28(4), 369-377, 2018. https://doi.org/10.15625/0868-3166/28/4/12683.

[4] Seekaew, Y., Pon-On, W., & Wongchoosuk, C. Ultrahigh selective room-temperature ammonia gas sensor based on tin–titanium dioxide/reduced graphene/carbon nanotube nanocomposites by the solvothermal method. ACS omega, 4(16), 16916-16924, 2019. https://doi.org/10.1021/acsomega.9b02185.

[5] Su, P. G., & Yang, L. Y. NH3 gas sensor based on Pd/SnO2/RGO ternary composite operated at room-temperature. Sensors and Actuators B: Chemical, 223, 202-208, 2016. https://doi.org/10.1016/j.snb.2015.09.091.

[6] Armitage, B. I., Murugappan, K., Lefferts, M. J., Cowsik, A., & Castell, M. R. Conducting polymer percolation gas sensor on a flexible substrate. Journal of Materials Chemistry C, 8(36), 12669-12676, 2020. https://doi.org/10.1039/D0TC02856H.

[7] Murugappan, K., & Castell, M. R. Bridging electrode gaps with conducting polymers around the electrical percolation threshold. Electrochemistry Communications, 87, 40-43, 2018. https://doi.org/10.1016/j.elecom.2017.12.019.

[8] Pang, Z., Yildirim, E., Pasquinelli, M. A., & Wei, Q. Ammonia sensing performance of polyaniline-coated polyamide 6 nanofibers. ACS omega, 6(13), 8950-8957, 2021. https://doi.org/10.1021/acsomega.0c06272.

[9] Mkhize, N., Murugappan, K., Castell, M. R., & Bhaskaran, H. Electrohydrodynamic jet printed conducting polymer for enhanced chemiresistive gas sensors. Journal of Materials Chemistry C, 9(13), 4591-4596, 2021. https://doi.org/10.1039/D0TC05719C.

[10] Cheng, S., Wang, Y., Zhang, R., Wang, H., Sun, C., & Wang, T. Recent Progress in Gas Sensors Based on P3HT Polymer Field-Effect Transistors. Sensors, 23(19), 8309, 2023. https://doi.org/10.3390/s23198309.

[11] Kuo, C. G., Chen, J. H., Chao, Y. C., & Chen, P. L. Fabrication of a P3HT-ZnO nanowires gas sensor detecting ammonia gas. Sensors, 18(1), 37, 2017. https://doi.org/10.3390/s18010037.

[12] Duong, D. T., Wang, C., Antono, E., Toney, M. F., & Salleo, A. The chemical and structural origin of efficient p-type doping in P3HT. Organic Electronics, 14(5), 1330-1336, 2013. https://doi.org/10.1016/j.orgel.2013.02.028.

[13] Wang, W., Chen, C., Tollan, C., Yang, F., Qin, Y., & Knez, M. Efficient and controllable vapor to solid doping of the polythiophene P3HT by low temperature vapor phase infiltration. Journal of Materials Chemistry C, 5(10), 2686-2694, 2017. https://doi.org/10.1039/C6TC05544C.

[14] Li, G., Zhu, R., & Yang, Y. Polymer solar cells. Nature photonics, 6(3), 153-161, 2012. https://doi.org/10.1038/nphoton.2012.11.

[15] Park, Y. D., Cho, J. H., Kim, D. H., Jang, Y., Lee, H. S., Ihm, K., & Cho, K. Energy-level alignment at interfaces between gold and poly (3-hexylthiophene) films with two different molecular structures. Electrochemical and solid-state letters, 9(11), G317, 2006. https://doi.org/10.1149/1.2337862.

[16] Karthik, P., Ravichandran, S., Sasikala, V., Prakash, N., Mukkannan, A., & Rajesh, J. Effective photodegradation of organic water pollutants by the facile synthesis of Ag2O nanoparticles. Surfaces and Interfaces, 10, 3088, 2023. https://doi.org/10.1016/j.surfin.2023.103088.

[17] E Sultan, A., I Abdullah, H., & H Niama, A. Synthesis of Silver Oxide Nanoparticles using Different Precursor and Study Cytotoxicity Against MCF-7 Breast Cancer Cell line. Nanomedicine Research Journal, 8(3), 259-267, 2023. https://doi.org/10.22034/nmrj.2023.03.004.

[18] Shume, W. M., Murthy, H. A., & Zereffa, E. A. A review on synthesis and characterization of Ag2O nanoparticles for photocatalytic applications. Journal of Chemistry, 1, 15, 2020. https://doi.org/10.1155/2020/5039479

[19] De Freitas, J.N., Maubane, M.S., Bepete, G., van Otterlo, W.A., Coville, N.J. & Nogueira, A.F. Synthesis and characterization of single wall carbon nanotube-grafted poly (3-hexylthiophene) and their nanocomposites with gold nanoparticles. Synthetic metals, 176, 55-64, 2013. https://doi.org/10.1016/j.synthmet.2013.05.026.

[20] Keru, G., Ndungu, P. G., Mola, G. T., & Nyamori, V. O. Bulk heterojunction solar cell with nitrogen-doped carbon nanotubes in the active layer: effect of nanocomposite synthesis technique on photovoltaic properties. Materials, 8(5), 2415-2432, 2015. https://doi.org/10.3390/ma8052415.

[21] Hernández-Martínez, D., Nicho, M. E., Alvarado-Tenorio, G., García-Carvajal, S., Castillo-Ortega, M. M., & Vásquez-López, C. Elaboration and characterization of P3HT–PEO–SWCNT fibers using the electrospinning technique. SN Applied Sciences, 2, 1-9, 2020. https://doi.org/10.1007/s42452-020-2278-2.

[22] López-Mata, C., Nicho, M. E., Altuzar-Coello, P., del Angel-Meraz, E., García-Escobar, C. H., & Cadenas-Pliego, G. Synthesis and characterization of SWNTs/P3OT composites through in situ microwave-assisted polymerization. Journal of Materials Science: Materials in Electronics, 26, 7341-7350, 2015. https://doi.org/10.1007/s10854-015-3363-y.

[23] Mahakul, P. C., & Mahanandia, P. Structural and electrical characteristics of solution processed P3HT-carbon nanotube composite. In IOP Conference Series: Materials Science and Engineering 178 (1), 012024, 2017. IOP Publishing. https://doi.org/10.1088/1757-899X/178/1/012024.

[24] Musumeci, A. W., Silva, G. G., Liu, J. W., Martens, W. N., & Waclawik, E. R. Structure and conductivity of multi-walled carbon nanotube/poly (3-hexylthiophene) composite films. Polymer, 48(6), 1667-1678, 2007. https://doi.org/10.1016/j.polymer.2007.01.027

[25] Giulianini, M., Waclawik, E. R., Bell, J. M., Scarselli, M., Castrucci, P., De Crescenzi, M., & Motta, N. Microscopic and spectroscopic investigation of poly (3-hexylthiophene) interaction with carbon nanotubes. Polymers, 3(3), 1433-1446, 2011. https://doi.org/10.3390/polym3031433.

[26] O'Connell, M. J., Boul, P., Ericson, L. M., Huffman, C., Wang, Y., Haroz, E., ... & Smalley, R. E. Reversible water-solubilization of single-walled carbon nanotubes through polymer wrapping. Chemical physics letters, 342(3-4), 265-271, 2001. https://doi.org/10.1016/S0009-2614(01)00490-0.

[27] Giulianini, M., Waclawik, E. R., Bell, J. M., De Crescenzi, M., Castrucci, P., Scarselli, M., & Motta, N. Regioregular poly (3-hexyl-thiophene) helical self-organization on carbon nanotubes. Applied Physics Letters, 95(1), 20-31, 2009. https://doi.org/10.1063/1.3173825.

[28] Tiwari, D.C., Atri, P. & Sharma, R. Sensitive detection of ammonia using reduced graphene oxide/polypyrrole nanocomposites. Synthetic Metals, 203, 228-234, 2015. https://doi.org/10.1016/j.synthmet.2015.02.026.

[29] Yan, K., Toku, Y., Morita, Y. & Ju, Y. Fabrication of a multiwall carbon nanotube sheet-based hydrogen sensor on a stacking multi-layer structure. Nanotechnology, 29, 375503, 2018. DOI: 10.1088/1361-6528/aace96.